www.sciencemag.org/content/343/6169/432/suppl/DC1

Supplementary Materials for

Adaptation of Innate Lymphoid Cells to a Micronutrient Deficiency Promotes Type 2 Barrier Immunity

S. P. Spencer, C. Wilhelm, Q. Yang, J. A. Hall, N. Bouladoux, A. Boyd, T. B. Nutman, J. F. Urban Jr., J. Wang, T. R. Ramalingam, A. Bhandoola, T. A. Wynn, Y. Belkaid*

*Corresponding author. E-mail: ybelkaid@niaid.nih.gov

Published 24 January 2014, *Science* **343**, 432 (2014)
DOI: 10.1126/science.1247606

This PDF file includes

Materials and Methods

Mice.

C57BL/6 (WT), *Rag1*$^{-/-}$, *Rag2*$^{-/-}$*gc*$^{-/-}$, *IL-13*$^{-/-}$ and C57BL/6 germ-free mice were purchased from Taconic Farms. All mice were bred and maintained under pathogen-free conditions at an American Association for the Accreditation of Laboratory Animal Care accredited animal facility at the NIAID and housed in accordance with the procedures outlined in the Guide for the Care and Use of Laboratory Animals under an animal study proposal approved by the NIAID Animal Care and Use Committee. All mice were used between 6 and 13 weeks of age.

Generation of RARa$^{fl/fl}$ mice.

RARa$^{fl/fl}$ mice were generated using a similar targeting strategy previously described[35]. In brief the targeting vector was generated using BAC clones from the C57BL/6J RPCI-23 BAC library carrying exon 3 of the RARA gene flanked by LoxP sites. The construct was transfected into TaconicArtemis C57BL/6N Tac ES cell line. Correctly targeted ES cells were injected into Balb/c blastocysts to screen for chimerism. Chimeric mice where bred to C57BL/6 females and subsequent to Flp-deleter mice to remove positive selection markers.

Diet Studies.

Vitamin A-deficient (TD.10991) and -sufficient (20,000 IU vitamin A/kg, TD.10992) diets were purchased from Harlan Teklad Diets. At day 14.5 of gestation, pregnant females were administered either vitamin A-deficient or -sufficient diet and maintained on diet until weaning of litter. Weanlings were maintained on special diet throughout study.

Cell isolation from the lamina propria and Flow Cytometry.

Cells from small and large intestinal lamina propria (Lp) were prepared as previously described[36]. Single-cell suspensions were stained with CD16/32 (eBioscience) and with fluorochrome-conjugated antibodies against any combination of the following surface antigens: CD4, CD8α, CD11b, CD11c, DX5, CD49b, TCR-β, TCR-$\gamma\delta$, CD19, Ter119, NK1.1, Gr-1 and Thy1.2. Prior to fixation Live/Dead Fixable Blue Cell Stain Kit (Invitrogen) was used to exclude dead cells. For examination of transcription factors and cellular proliferation, cells were subsequently treated with the FOXP3 staining kit (eBioscience) in accordance with the manufacturer's instructions and stained for 20 min at room temperature with fluorochrome-conjugated antibodies against the following: RORgt, GATA3 and Ki67. (clone numbers are listed in table S1 and gating strategies are supplied in Fig. S22)

Intracellular cytokine staining.

Isolated cells from lamina propria were stimulated for 2 h with phorbol 12-myristate 13-acetate (PMA) (50ng/ml) and ionomycin (2.5μg/ml) in the presence of Brefeldin A (1μg/ml) (GolgiPlug, BD Biosciences).

Cell isolation from the lung and skin.

Tissues were diced followed by digestion with 0.25mg/ml liberase TL (Roche) at 37˚C for 45 min (lung) or liberase and 1mg/ml DNase at 37˚C for 1h 15min (skin). Isolated lung cells were further purified using a 37.5% Percoll gradient followed by lysis of red blood cells with ACK.

Fluorescence-activated cell sorting and *in vitro* culture of ILC and ILC2P.

ILC3 were sorted by flow cytometry from small intestine Lp cells from WT and VAI mice based on the absence of lineage markers (CD4, CD8α, CD11b, CD11c, DX5, CD49b, TCR-β, TCR-$\gamma\delta$, CD19, Ter119, NK1.1 and Gr-1) but expression of

Thy1.2 and IL-7R. ILC2 were sorted as lineage negative, Thy1.2^{+}, KLRG1^{+}. ILC2 progenitors (ILC2P) were sorted from the bone marrow of Rag1$^{-/-}$ mice by the absence of lineage makers and c-Kit, but expression of IL-7R, CD25 and high levels of Sca-1[37-39]. RPMI 1640 supplemented with 10% FBS, penicillin, streptomycin, HEPES, glutamine, nonessential amino acids, and 50 mM of β-mercaptoethanol (Complete Media) was used for *in vitro* culture. ILC2 (5x10^3 cells), ILC3 (10x10^3 cells) or ILC2P (2.4x10^3 cells) were cultured in 50μl in the presence of IL-7 (10ng/ml) and/or SCF (10ng/ml) in the presence or absence of 1 μM all-trans RA (Sigma-Aldrich) or 1.8 μM RA inhibitor BMS 493 (Tocris, UK) for 3 days or 7 days in the case ILC2p respectively. Cytokine expression in the cell free supernatant was assessed using a bead based cytokine detection assay (FlowCytomix, eBioscience) and was adjusted to the plated density of 5x10^3 cells in 50 *μ*l culture volume.

Retrovirus transduction and adoptive transfer of bone marrow progenitors.

Bone marrow LSK (Lin$^-$ Sca-1$^+$Kit$^+$, CD45.2) were sorted, cultured with 6 ng/ml IL-3, 5 ng/ml IL-6 and 100 ng/ml SCF and transduced with MSCV-CRE-GFP retrovirus using retronectin (Takara) according to the manufacturer's instructions. After 24h, 2x10^5 cells were injected intravenously into lethally irradiated (950 rads) CD45.1 recipient mice. The recipient mice were treated with 250 *μ*g retinoic acids in 30*μ*l DMSO Intraperitoneally at day 0, day 4 and day 8 post-transplant. Mice were analyzed at 3 weeks post-transplant.

Real time PCR.

Tissues were homogenized using metal beads (Precellys). RNA was extracted using RNAeasy mini kit (Qiagen) and reverse transcribed with Omniscript (Qiagen) according to the manufacturer's intructions. The cDNA served as template for the amplification of genes of interest and the housekeeping gene (*b-actin*) by real-time PCR using SYBR green. Target gene expression was calculated using the comparative method for relative quantification upon

normalisation to *b-actin* gene expression. Primer sequences: (*actb*: 5'-AAGTGTGACGTTGACATCCGTAA-3' and 5'-TGCCTGGGTACATGGTGGTA-3'; *retnlb*: 5'-ATGGGTGTCACTGGATGTGCTT-3' and 5'-AGCACTGGCAGTGGCAAGTA-3'). For analysis of genes expressed on ILC TaqMan® probes for *RARa, RARb, RARg* (Life technologies) were used and gene expression was normalized to *hprt1.*

In Vivo retinoic acid inhibitor (BMS493) treatment and RA Reconstitution.

A total of 220µg of the pan retinoic acid receptor inverse agonist BMS 493 (R&D) resuspended in 30 µl of biotechnology performance certified DMSO (Sigma Aldrich) was administered intraperitoneally to *Rag1*$^{-/-}$ mice every day for 8 days as previously described[18]. Control mice received DMSO only. In some experiments *Rag1–/–* mice were treated with RAi for 5 days followed by infection with *C.rodentium*. Injection of RAi or DMSO continued until the mice were sacrificed but not longer than 14 days of total treatment. In some case mice were simultaneously administered with 400ng of anti-IL-7Ra antibody every 4 days intraperitoneally to block IL-7Ra signaling. A total of 250 µg of all-trans-RA (Sigma Aldrich) in 30 µl of biotechnology performance certified DMSO (Sigma Aldrich) was administered intraperitoneally to VAI mice every other day for 12 days. Mice not receiving RA received DMSO vehicle.

Infection with *Citrobacter rodentium.*

For *C. rodentium* infections (formerly *Citrobacter freundii*, biotype 4280) strain DBS100 (provided by David Artis, University of Pennsylvania, Philadelphia, Pennsylvania, USA) was prepared by selecting a single colony and culturing in LB broth for 8 hours. Mice pre-treated for 5 days with vehicle control or RAi were inoculated with approximately 1×10^{10} CFU in 200 µL of PBS via oral gavage. In some cases VAI mice were treated with 400ng of recombinant mouse IL-22 (rmIL-22, Biolegend) intraperitoneally every day for 4 days starting 2 days before

infection. Treatment with rmIL-22 continued every other day from day 2 after infection until mice were sacrificed.

Infection with *Trichuris muris.*

Mice were inoculated with 25-30 (low dose) or 150 (high dose) infective *Trichuris muris* eggs on day 0 by oral gavage, and 12-14 days later infected mice were sacrificed and their worm burden was assessed in the cecal epithelial cell layer. C57Bl/6 WT mice were simultaneous treated with vehicle or RAi every day starting upon infections with *T. muris*. In some cases VAI mice were simultaneous treated with 500ng of anti-IL-13 antibody[40] intraperitoneally every 5 days for up to 12 days.

Goblet cells scoring in the small intestine.

Sections of the small intestine of control mice or VAI mice were stained with periodic acid-schiff (PAS). 5-10 villi per slide were assessed for PAS positive goblet cells. A total of 2 slides distributed over 3 randomly selected areas were counted. In some cases VAI mice were treated with 500ng of anti-IL-13 antibody[40] intraperitoneally every 5 days for up to two weeks.

Statistical analysis.

A two-tailed Student's *t*-test was used for all statistical analysis, * $p \leq 0.05$, ** $p \leq 0.005$, *** $p \leq 0.0005$.

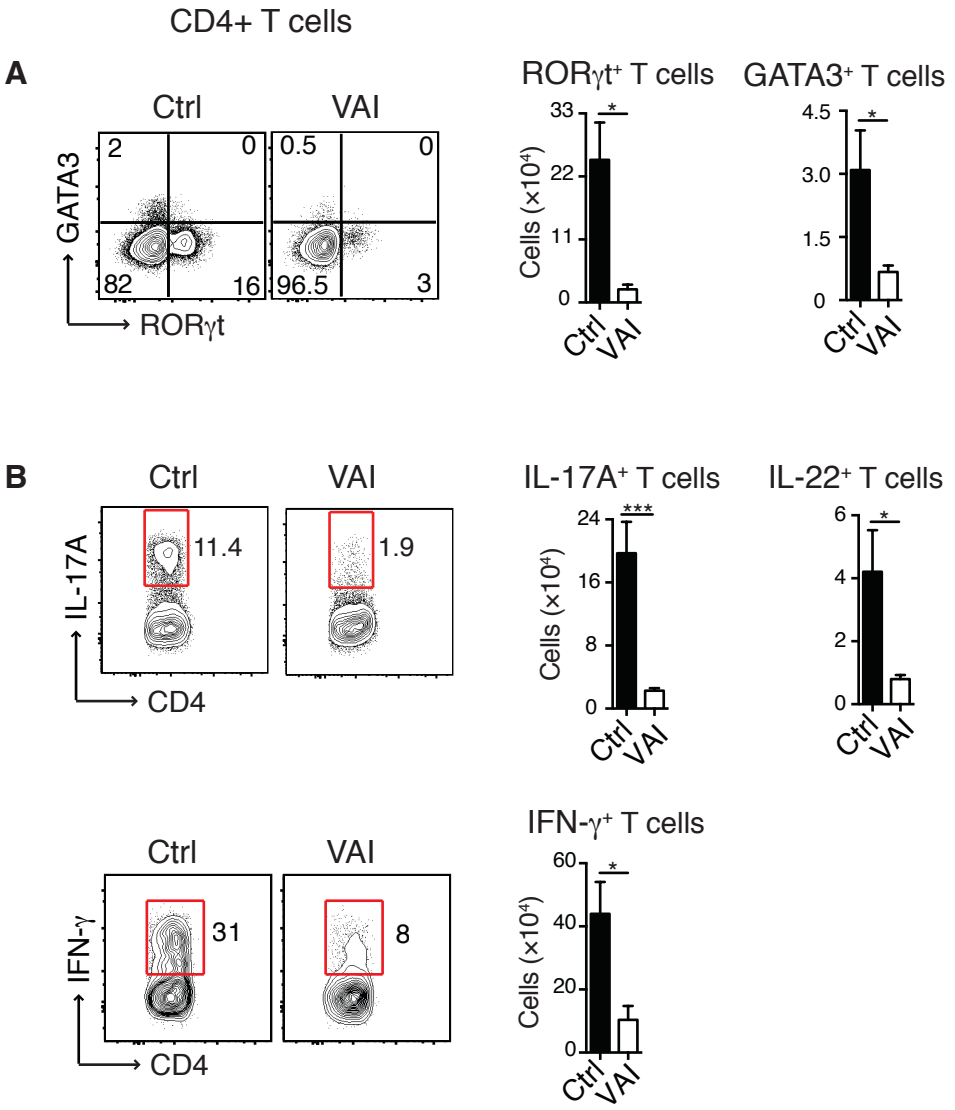

Fig. S1.

Reduction of steady state Th17 and Th1 in vitamin A insufficient mice. **A**) Cells isolated from the small intestine lamina propria (SiLP) of control or VAI mice gated on CD4$^+$ Foxp3$^-$ T cells and analyzed for GATA3 and RORγt (left panel) and total number of RORγt$^+$ T cells (Th17) and GATA3$^+$ T cells (Th2) (right panel). **B**) Flow analysis of SiLP cells stimulated with PMA and ionomicin for 2.5 h, gated on CD4$^+$ T cells and analyzed for intracellular IL-17A, IL-22 and IFN-γ expression (left panels) and total numbers of IL-17A, IL-22 and IFN-γ producing CD4$^+$ T cells in the small intestine (right panel). Data represent two independent experiments with 3-5 mice in each experimental group. (Graphs display mean ±SEM).

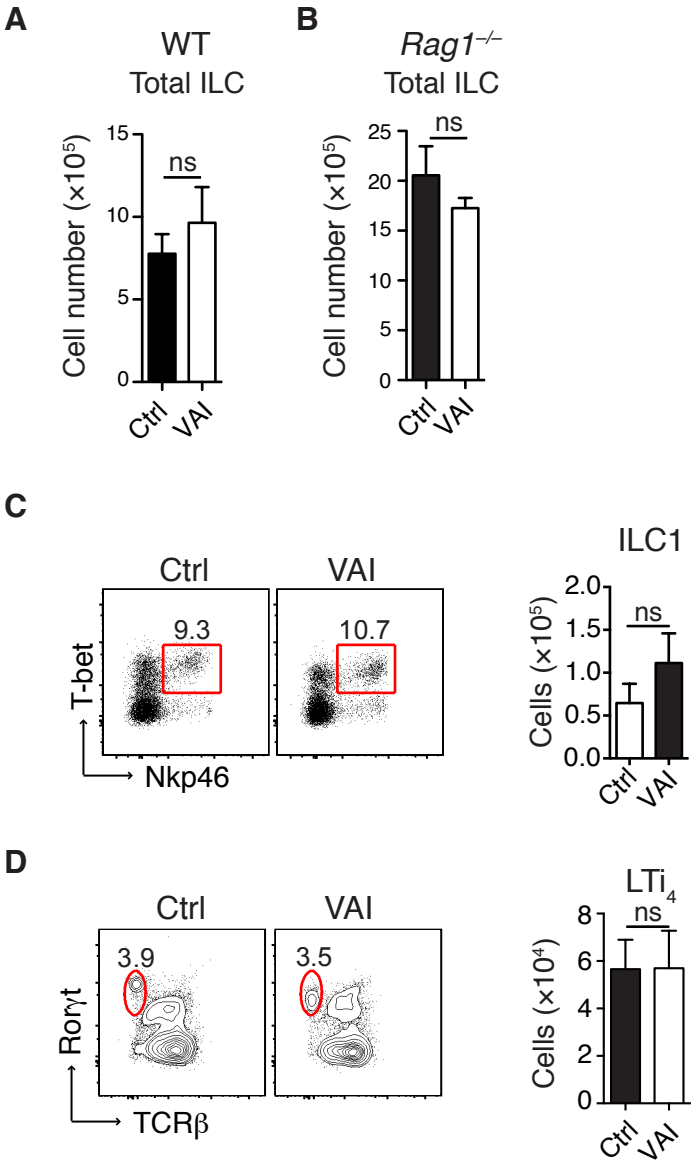

Fig. S2.

Total numbers and composition of small intestinal ILC in vitamin A insufficient mice. Cells were isolated from the small intestinal lamina propria (SiLP) from control (Ctrl) or vitamin A insufficient (VAI) WT and Rag1$^{-/-}$ mice. **A)** Total numbers of ILC in WT and **B)** Rag1$^{-/-}$ VAI mice. Cells were isolated from the SiLP of WT and VAI mice and **C)** gated on TCRβ^{-}, RORγt^{-} and Gata3^{-} and analyzed for T-bet and Nkp46 expression (left panel) and total numbers of ILC1 (right panel). **D)** SiLP cells were gated on Thy1.2^{+} and CD4^{+} cells and analyzed for RORγt^{+} TCRβ^{-} LTi(left panel) and total numbers of LTi$_4$. Data represent at least two **(A-C)** or four **(D)** independent experiments with 3-5 mice in each experimental group (Graphs mean ±SEM)

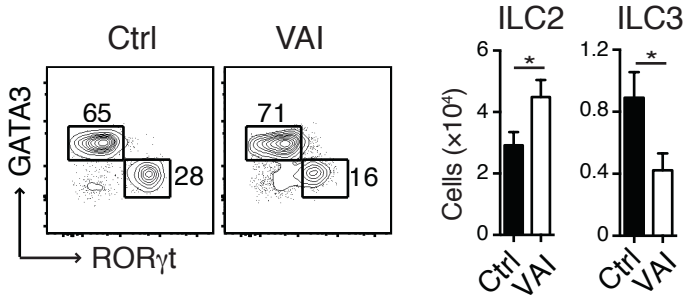

Fig. S3.

Inverse regulation of ILC subsets by vitamin A in the colon. Cells were isolated from the lamina propria of the colon in WT and VAI mice and analyzed by flow cytometry. RORγt and GATA3 expression in ILC (Lin-, Th1.2^{+}) (left panel) and total numbers of ILC in the large intestine (right panel). Data represent pooled results from two independent experiments with 3-5 mice in each experimental group (Graphs mean ±SEM).

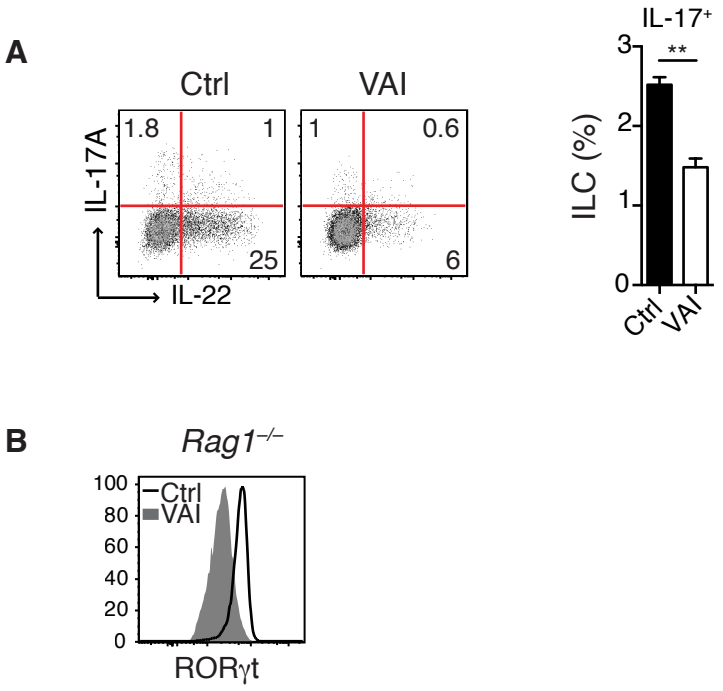

Fig. S4.

Composition of ILC observed in vitamin A insufficient mice. Cells were isolated from the small intestinal lamina propria (SiLP) from WT and VAI mice and analyzed by flow cytometry. **A)** Cells were gated on ILC (Lin^- $Thy1.2^+$ cells) and analyzed for the expression of intracellular IL-17A and IL-22 following stimulation with PMA and ionomycin (left panel) and frequencies of IL-17A expressing ILC (right panel). **B)** RORγt expression in ILC3 from Ctrl and VAI $Rag1^{-/-}$ mice. Data represent at least two independent experiments with 3-5 mice in each experimental group (Graphs mean ±SEM)

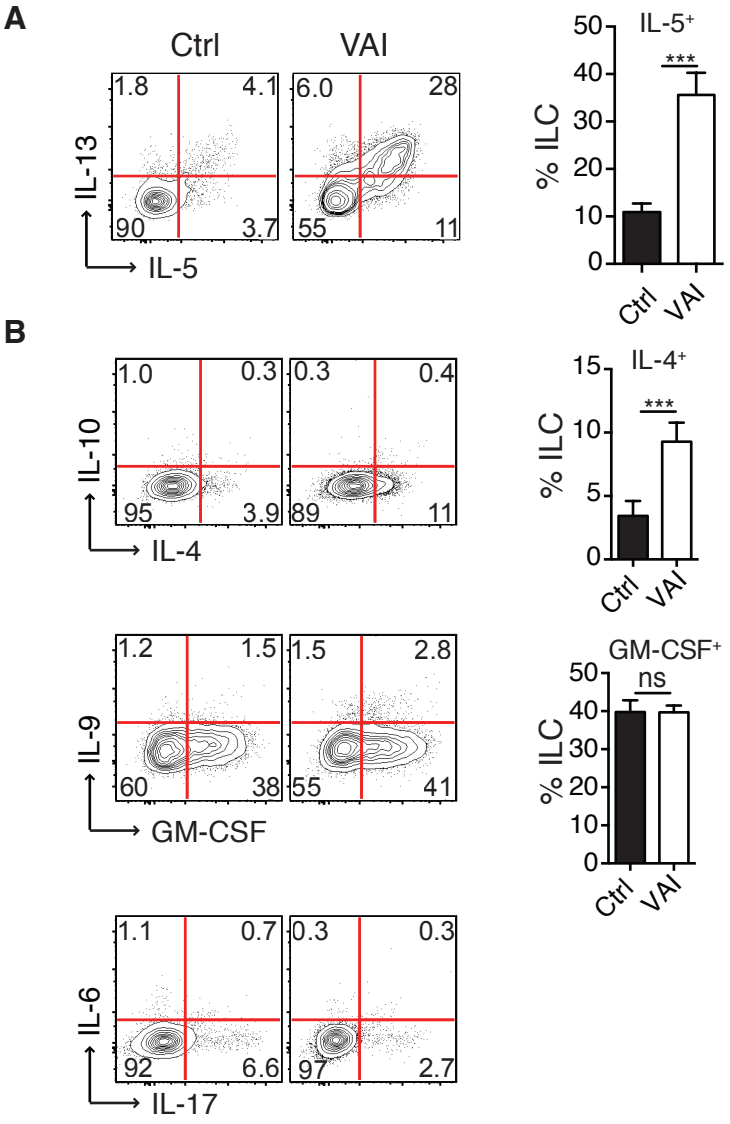

Fig. S5.

Cytokine expression from ILC in vitamin A deficient mice. Cells were isolated from the small intestinal lamina propria (SiLP) from WT and VAI mice, gated on ILC ($Lin^-Thy1.2^+$ cells) and analyzed for the expression of intracellular **A)** IL-5 and IL-13 cytokine expression following stimulation with PMA and ionomycin (left panel and frequencies of IL-5expressing ILC (right panel). **B)** Intracellular expression of cytokines in ILC from Ctrl and VAi mice (left panel) and frequencies of cytokine expressing ILC (right panel). Data represent two (**A**) or one (**B**) experiment with 3-5 mice in each experimental group. (Graphs mean ±SEM).

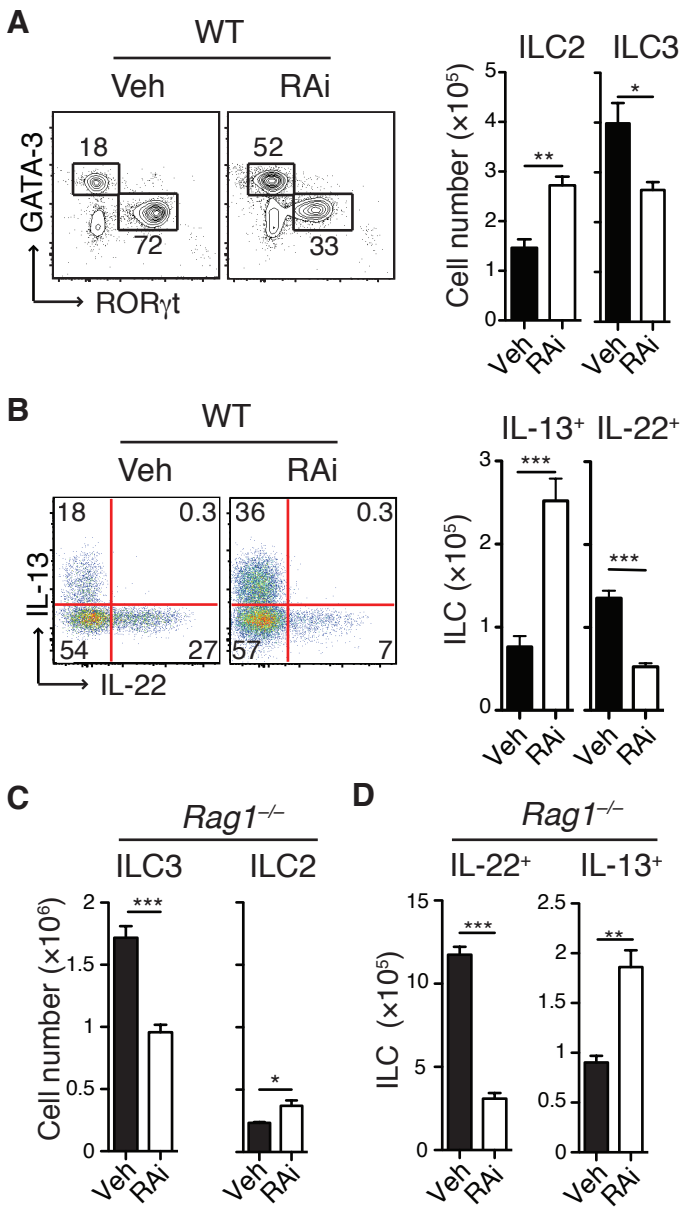

Fig. S6.

ILC number and cytokine production in the absence of RA signaling. A) Cells were isolated from the small intestinal lamina propria (SiLP) of WT mice **(A,B)** or Rag1$^{-/-}$ **(C,D)** treated with retinoic acid receptor inhibitor (RAi) or vehicle control (Veh) for 8 days were stained for GATA3 and RORγt and gated on Lin^{-} and Thy1.2^{+} cells (right panel) and total numbers of ILC3 (RORγt^{+}) and ILC2 (GATA3^{+}) (right panel) **B**) Flow cytometry of SiLP cells stimulated with PMA and ionomicin for 2h, gated on Lin- Thy1.2^{+} cells and analyzed for intracellular IL-13 and IL-22 expression (left panel) and total numbers of IL-22 and IL-13 producing ILC in the small intestine (right panel). **C**) Total number of ILC3 and ILC2 isolated from the SiLP of Rag1$^{-/-}$ mice treated with retinoic acid receptor inhibitor (RAi) or vehicle control (Veh) for 8 days **D**) Total numbers of IL-22 and IL-13 producing ILC in the small intestine. Data represent at least two independent experiments with 3-4 mice in each experimental group (Graphs display mean ±SEM).

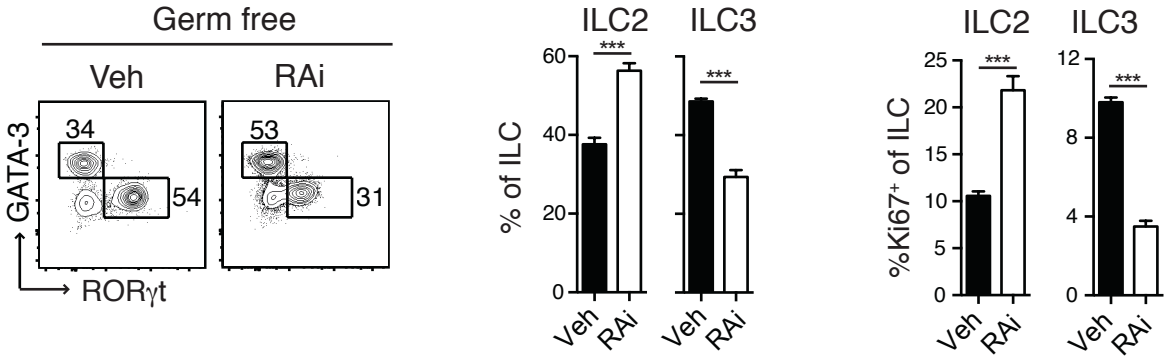

Fig. S7.

Inverse regulation of intestinal ILC subsets by RA signaling occurs independently of the microbiota. Cells were isolated from the small intestine lamina propria (SiLP) of germ free mice treated with retinoic acid receptor inhibitor (RAi) or vehicle control (Veh) for 8 days. GATA3 and RORγt expression in Lin^- and $Thy1.2^+$ cells(left panel) and frequencies of ILC3 ($ROR\gamma t^+$) and ILC2 ($GATA3^+$) cells (middle panel) and frequencies of $Ki67^+$ ILC (right panel). Data represent two independent experiments with 3-5 mice in each experimental group. (Graphs display mean ±SEM).

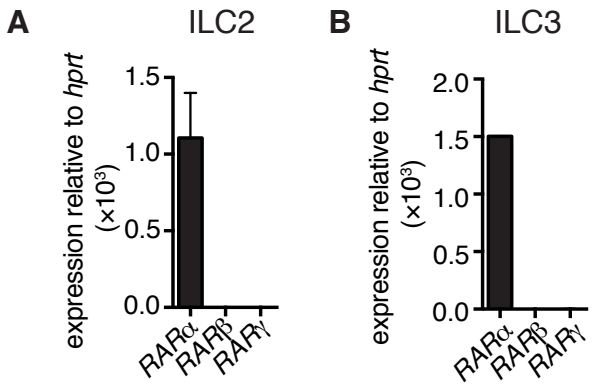

Fig. S8.
Expression of retinoic receptor α (RARα) in ILC2 and ILC3. Cells were isolated from the small intestine lamina propria (SiLP) of WT mice and ILC2 and ILC3 were purified by flow activated cells sorting. **A**) Relative mRNA expression of *Rar*α, –β and –γ in ILC2 and **B**) ILC3. Data represent one experiment with two seperate samples in each experimental group.

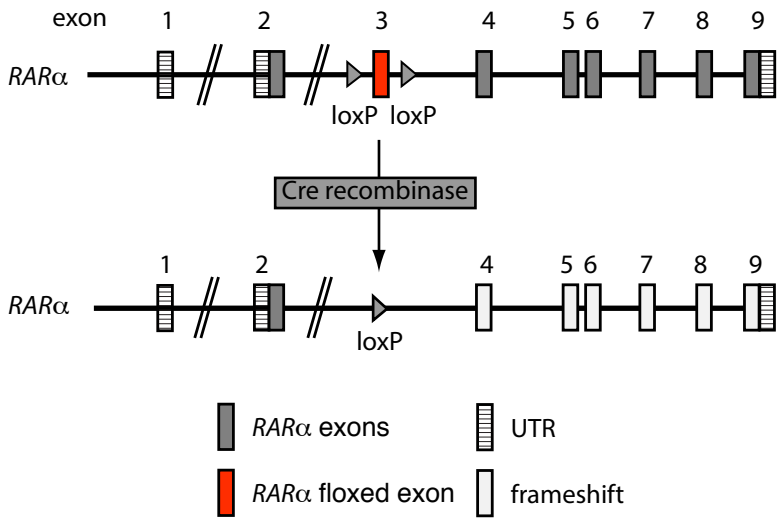

Fig. S9.
Generation of RARα$^{fl/fl}$ mice. A targeting vector was generated using BAC clones from the C57BL/6J RPCI-23 BAC library carrying exon 3 of the RARα gene flanked by LoxP sites . In addition the targeting vector contained positive selection markers flanked by FRT sites (Neomycin resistance-NeoR) and F3 (Puromycin resistance-PuroR) inserted into intron 2 and intron 3 respectively (not depicted). The construct was transfected into TaconicArtemis C57BL/6N Tac ES cell line. Correctly targeted ES cells were injected into Balb/c blastocysts to screen for chimerism. Chimeric mice where bred to C57BL/6 females and subsequent to Flp-deleter mice to remove both the Neo and Puro cassette. Expression of the Cre recombinase will allow for specific excision of exon 3 and will generate a frameshift from exon 2 to exon 4 with a premature Stop codon in exon 5 thus resulting in a functional loss of the RARα gene. A similar targeting strategy has been used before (Chapellier B et al. Genesis, 32, p 87-90, 2002). Schematic not drawn to scale.

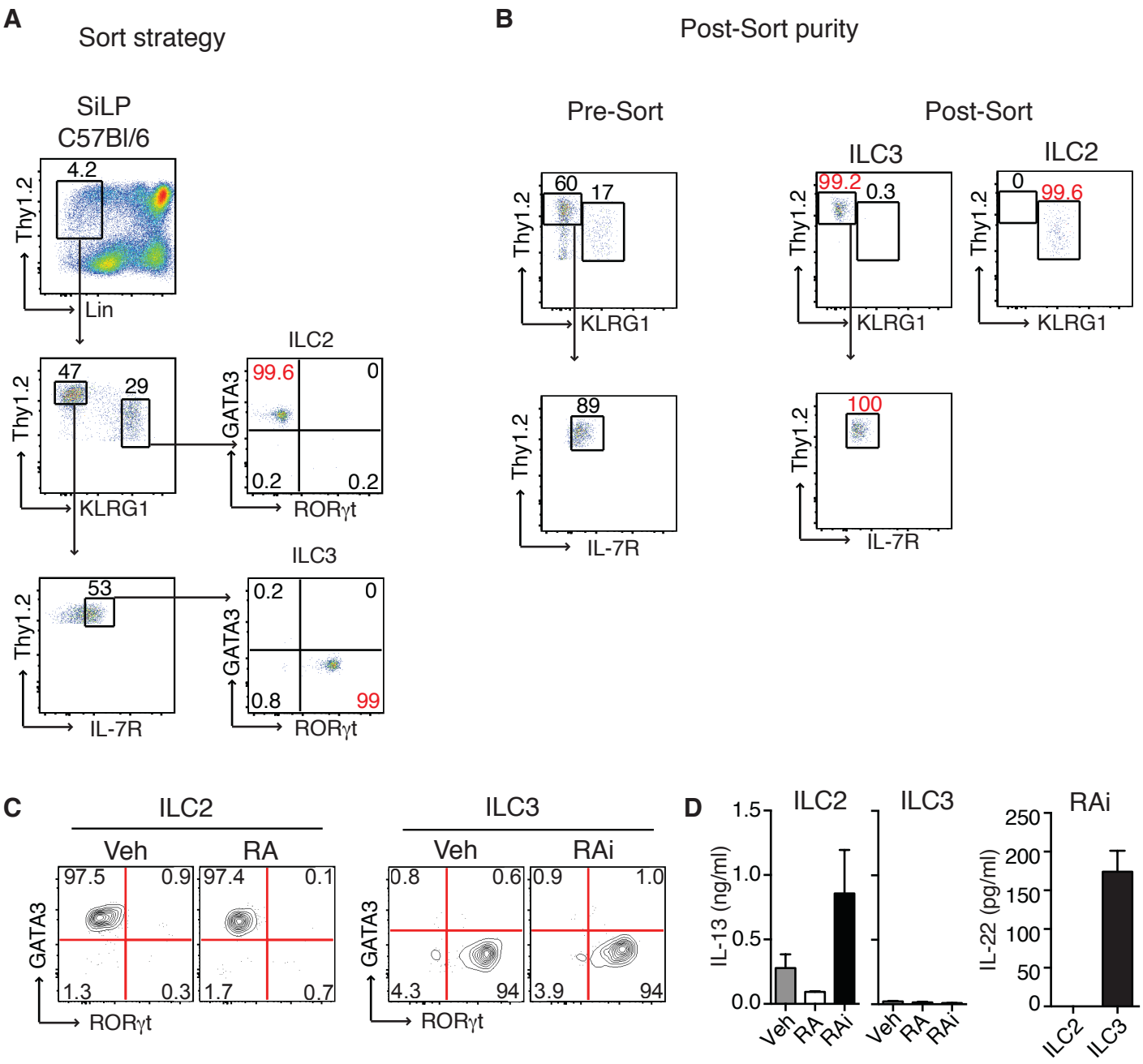

Fig. S10.

Sorting strategy for isolation of ILC populations and stability in culture in response to RA. A) SiLP cells were stained with lineage markers (NK1.1, TCRβ, TCRγδ, CD11b, CD11c, CD4, CD8a, CD8b, CD19, GR-1, DX5, Ter119) and Thy1.2 and gated on live and CD45+ cells. ILC2 were sorted as Thy1+, Lineage-, KLRG1+ and ILC3 were sorted as Thy1^{hi}, KLRG-, and IL-7R+ yeilding greater than 99% of cells expressing Gata-3 and Rorgt respectively. **B)** Post-sort purity measurements indicating greater than 99% purity of sorted populations. **C**) FACS purified ILC2 (left panel) and ILC3 (right panel) were cultured with vehicle control (Veh), retinoic acid (RA) or retinoic acid signaling inhibitor (RAi) in the presence of IL-7 for 3 days. **D**) IL-13 (left panel) and IL-22 (right panel) production of ILC2 and ILC3 in the presence of RA or RAi. Data represent two independent experiments. (Graphs display mean ±SEM).

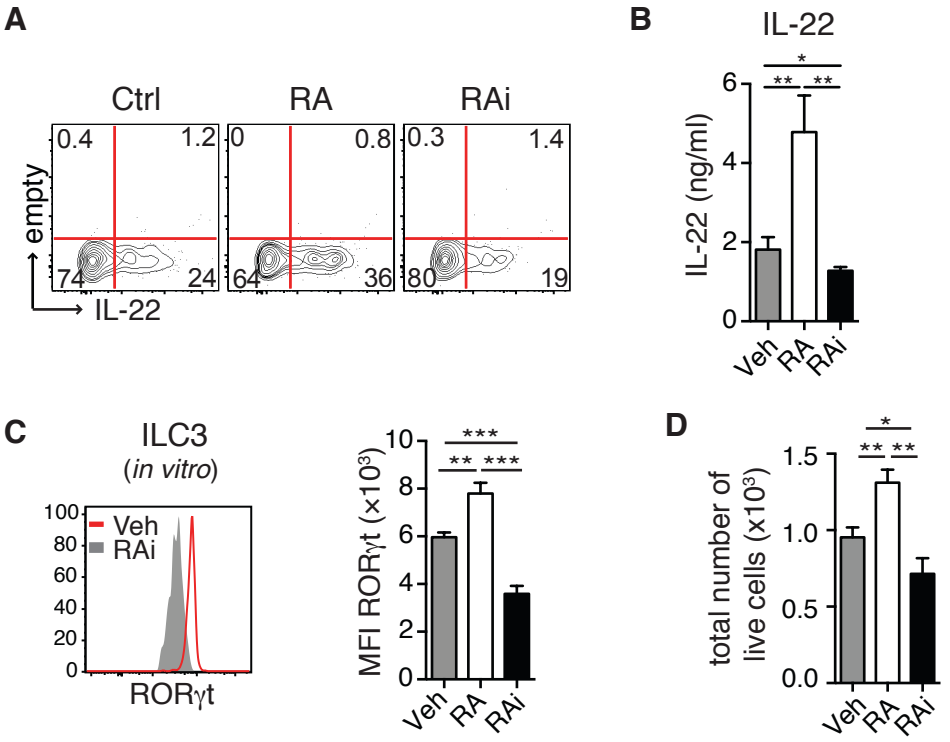

Fig. S11.
Retinoic acid effects ILC3 numbers and promotes IL-22 expression. A) Sort purified ILC3 cultured with IL-7 and vehicle, RA or RAi were stimulated with IL-1α and IL-1β for 6 hours in the presence of Brefeldin A and assessed for intracellular expression of IL-22. **B)** IL-22 contents in the culture supernatant of sort purified ILC3 cultured over night with IL-7 and vehicle, RA or RAi and stimulated with IL-1α and IL-1β for 24h. **C)** ILC3 were purified by fluorescent activated flow sorting (FACS) from small intestinal lamina propria (SiLP) of WT C57Bl/6 mice and cultured with Veh, RA or RAi in the presence of SCF(10ng/ml) for 3 days. RORγt+ expression (left panel) and mean fluorescent intensity of RORγt expression (right panel) and **D)** total number of live ILC3. Data are representative of at least two independent experiments with 3 experimental groups of cells isolated from 2 mice each (Graph is mean ±SEM).

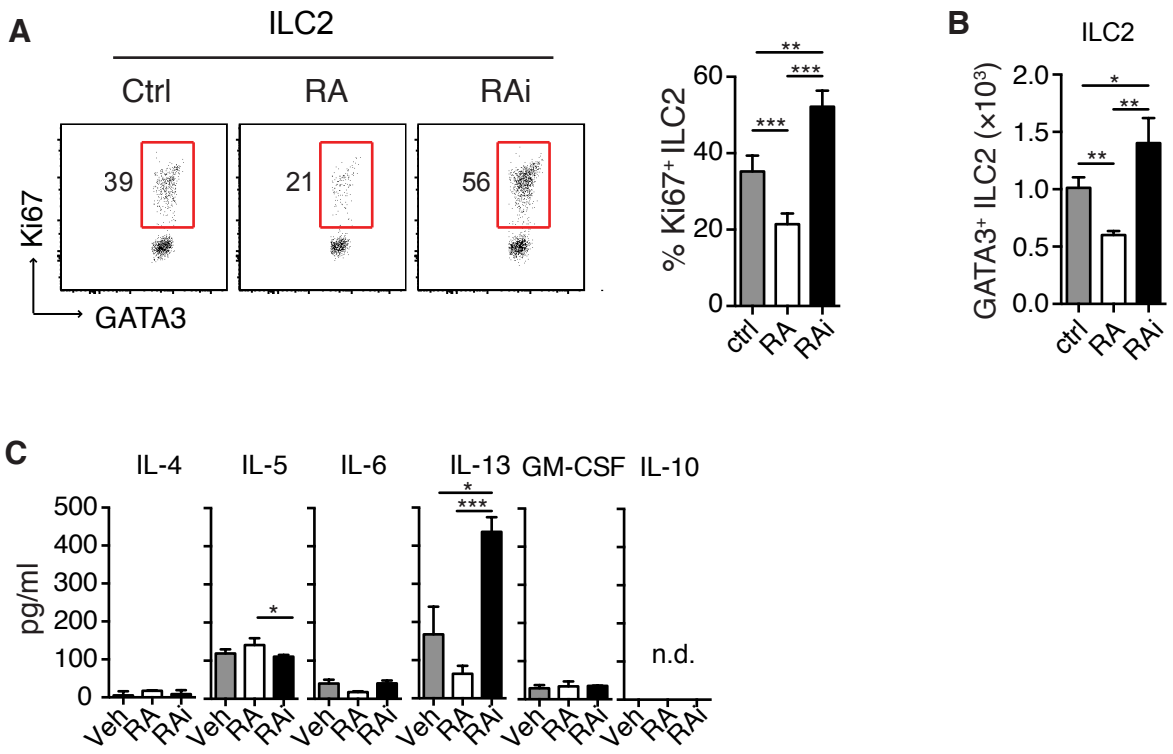

Fig. S12.
RA signaling inhibition augments ILC2 accumulation and IL-13 production. ILC2 were purified by fluorescent activated flow sorting (FACS) from small intestinal lamina propria (SiLP) cells WT mice and cultured with Veh, RA or RAi in the presence of IL-7 (10ng/ml) for 3 days. **A)** Ki67 expression in ILC2 (left panel) and quantification of frequencies of Ki67⁺ ILC2. **B)**Total numbers of GATA3⁺ ILC2 cultured in the presence of IL-7. **C)** Cytokine expression in the culture supernatant of cultured ILC2. Data represent two independent experiments with 3 independent groups of ILC2. (Graphs mean ±SEM).

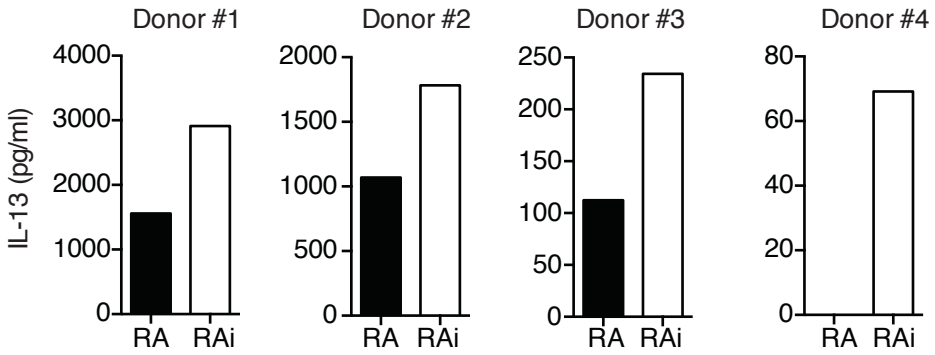

Fig. S13.

RA supresses IL-13 expression from human ILC2. PBMC were isolated from healthy donors and ILC (Lin-cKit+IL7R+) were sorted by FACS. Sorted ILC were cultured with RA or RAi in the presence of IL-7 (10ng/ml) and SCF (10ng/ml) for 7 days. IL13 was measured in the cell-free supernatant from cultured ILC adjusted to the plated density of $5x10^3$ cells in 50 µl culture volume. Data are representative of 4 independent human donors.

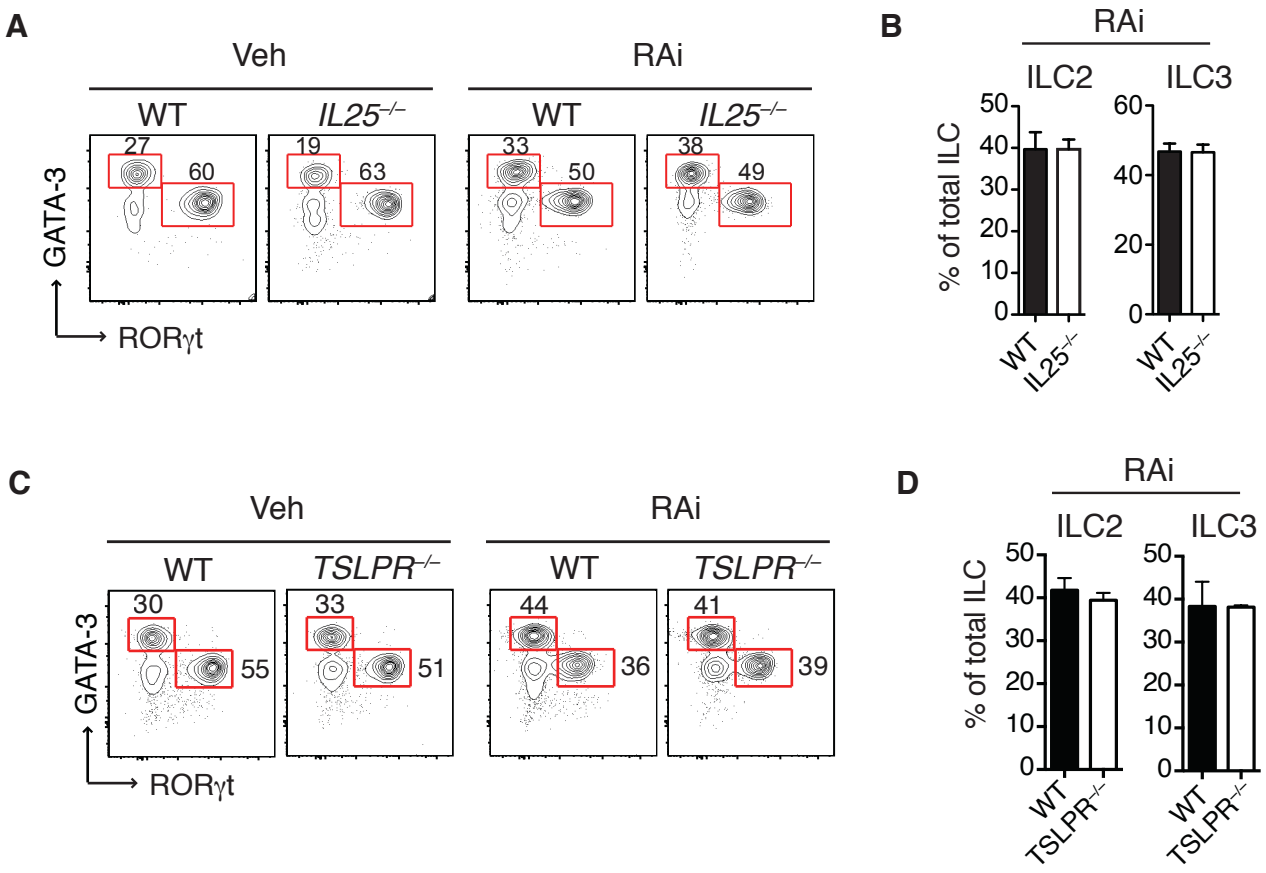

Fig. S14.

Inverse regulation of intestinal ILC subsets by RA occurs independent of IL-25 and TSLP. **A**) Cells isolated from the small intestine lamina propria (SiLP) of IL-25$^{-/-}$ mice or WT mice treated with retinoic acid receptor inhibitor (RAi) or vehicle control (Veh) for 8 days were stained for GATA3 and RORγt and gated on Lin^{-} and Thy1.2^{+} cells. **B**) Frequencies of ILC3 (RORγt^{+}) and ILC2 (GATA3^{+}) cells. **C**) RORγt^{+} and Gata3^{+} ILC in TSLP$^{-/-}$ mice and **D**) frequencies of ILC3 and ILC2. Data represent one experiment with 2-3 mice in each experimental group. (Graphs display mean ±SEM).

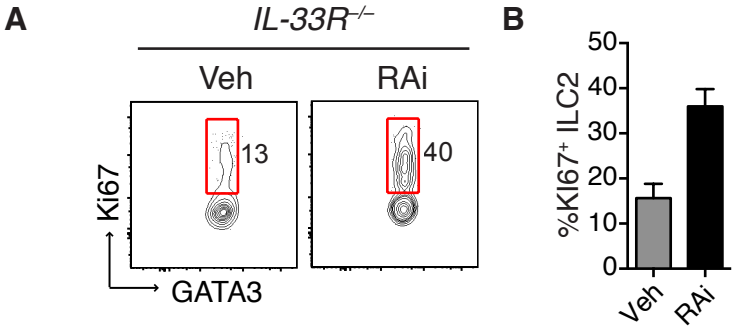

Fig. S15.

IL-33R is dispensable for increased Ki67 expresison in ILC2 in the absence of RA signaling . **A**) Cells isolated from the small intestine lamina propria (SiLP) of WT mice or IL-33R$^{-/-}$ mice and analyzed for Ki67 expression on ILC2. **B**) Frequencies of Ki67^{+} ILC2. Data represent two independent experiments with 2-3 mice in each experimental group. (Graphs display mean ±SEM).

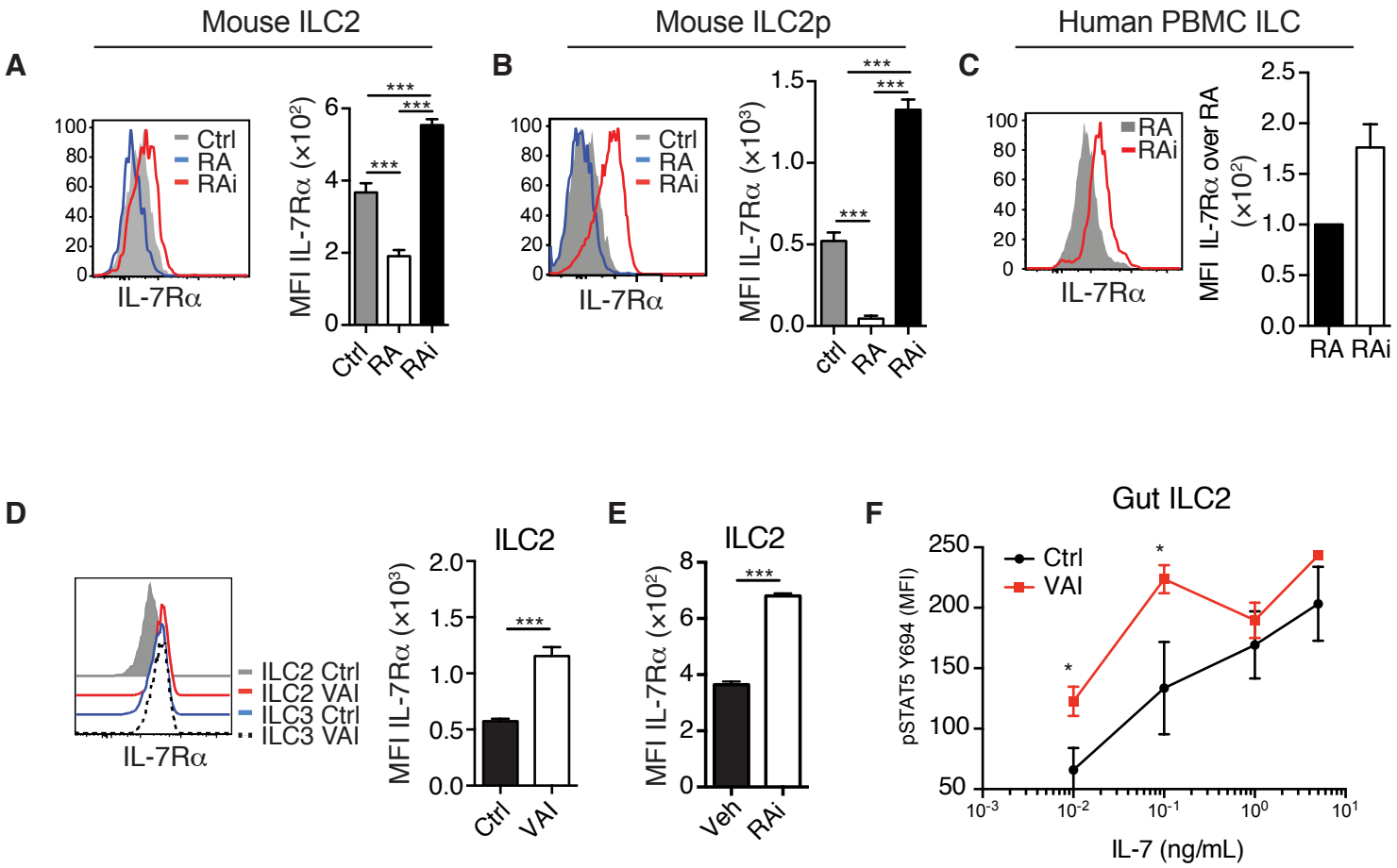

Fig. S16.

RA controls IL-7Rα expression in mouse and human ILC2. ILC2 were purified by fluorescent activated cell sorting from small intestine lamina propria (SiLP) cells and ILC2p from bone marrow cells of WT mice and cultured with Veh, RA or RAi in the presence of IL-7 (10ng/ml) for 3 days (ILC2) or IL-7 and SCF for 7 days (ILC2p). **A)** IL-7Rα expression on ILC2 after 3 days of culture (left panel) and MFI of IL-7Rα expression (right panel). **B)** IL-7Rα expression on ILC2p (left panel) and MFI of IL-7Rα expression (right panel). **C)** PBMC were isolated from different human donors and ILC were sorted by flow cytometry via the expression of ckit and IL-7Rα but the absence of lineage specific markers. IL-7Rα expression on Gata3^{+} ILC2 after 18 hours of culture with RA or RAi (left panel) and MFI of IL-7Rα normalized to ILC2 cultured with RA (right panel). **D)** IL-7Rα expression on ILC2 and ILC3 isolated from SiLP of control (Ctrl) or VAI mice (left panel) and MFI of IL-7Rα expression on ILC2 from Ctrl or VAI mice (right panel). **E)** MFI of IL-7Rα expression on ILC2 isolated from the SiLP of WT mice treated with RAi or vehicle control (Veh) for 8 days. **F)** MFI of phospho-STAT5 in ILC2 isolated from the SiLP of Ctrl or VAI mice stimulated with IL-7. Data represent at least two independent experiments with 3 experimental groups of sort purified ILC2 or ILC2p (**A-B**) or three (**D-E**) or one (**F**) independent experiments with 3-5 mice in each group or 4 independent human donors (**C**). (Graphs mean ±SEM)

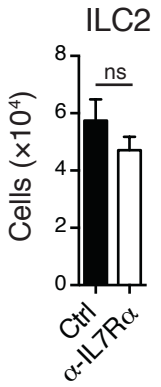

Fig. S17.
IL-7Rα blockade does not alter ILC2 numbers. Total number of ILC2 isolated from the small intestine lamina propria (SiLP) of mice treated with either PBS control (Ctrl) or anti α-IL7Rα every 4 days for 8 days. ILC2 were quantified. Results represent one-experiment with 3 mice per group. (Graphs mean ±SEM).

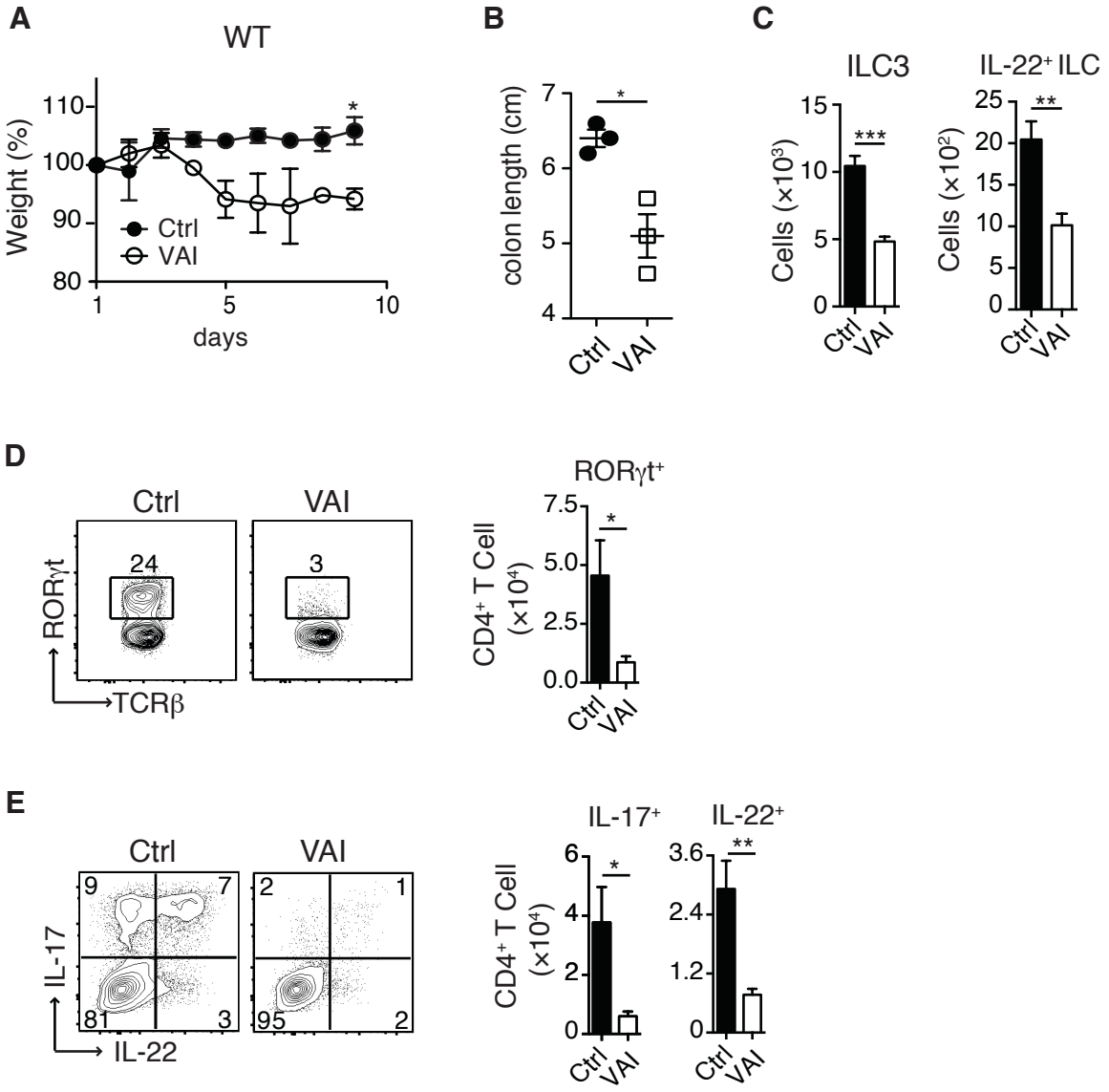

Fig. S18.

Enhanced *Citrobacter rodentium* infection induced pathology and impaired Th17 and ILC3 responses in the absence of vitamin A. A) Percentile change of original body weight and **B)** colon length of vitamin A insufficient (VAI) and control (Ctrl) C57Bl/6 mice infected with *C. rodentium* at Day 9. Large intestinal lamina propria cells were isolated from control (Ctrl) or vitamin A insufficienct (VAI) mice 9 days after oral infection with *C. rodentium*. **C**)Total amount of ILC3 and IL-22 expressing ILC. **D**) Cells were gated on $CD4^+$ $TCR\beta^+$ $Foxp3^-$ cells and analyzed for intracellular $ROR\gamma t$ (left panel) and total numbers of $Foxp3^-ROR\gamma t^+$ $CD4^+$ T cells (Th17) (right panel). **E**) IL-17 and IL-22 expression after PMA/Iono stimulation (left panel) and total amount of IL-17 and $IL\text{-}22^+$ expressing $CD4^+$ T cells (right panel). Data represent at least two experiments with 3-5 mice in each experimental group. (Graphs mean ±SEM)

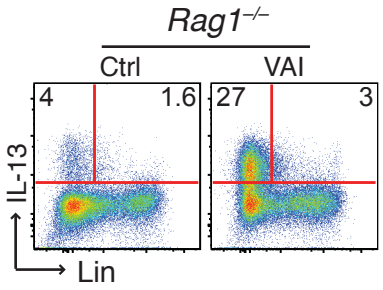

Fig. S19.
ILC are the dominant source of IL-13 in VAI *RAG1*$^{-/-}$ mice. Cells isolated from the small intestine lamina propria (SiLP) from control (Ctrl), vitamin A insufficient (VAI) *Rag1*$^{-/-}$ mice stimulated with PMA and ionomicin for 2h, gated on CD45^{+} cells, stained for lineage markers and intracellular IL-13. Data represents three independent experiments.

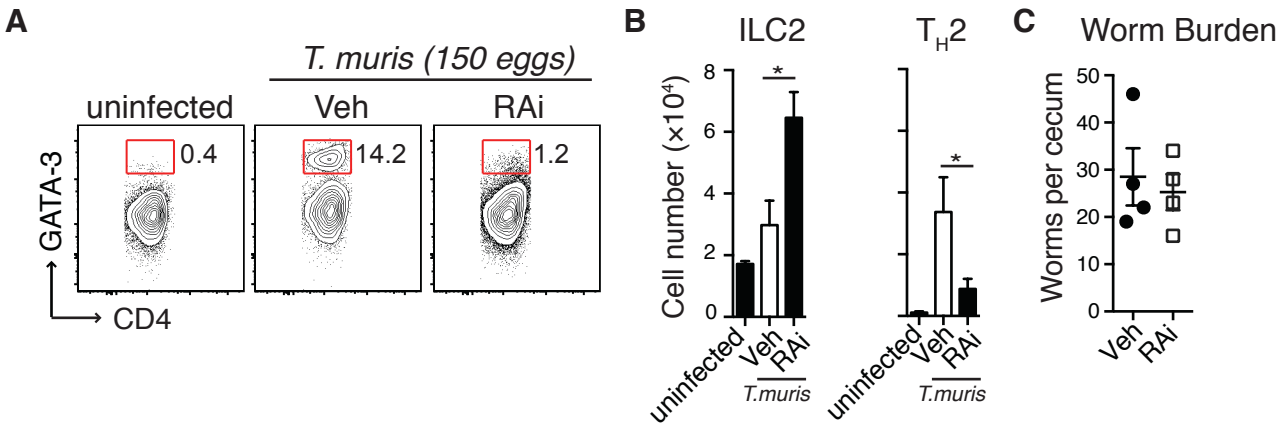

Fig. S20.
Diminished Th2 response in the absence of RA signaling in response to high dose infection with *T. muris*. WT mice treated every other day with retinoic acid receptor inhibitor (RAi) or vehicle control (Veh) for 14 days after oral infection with 150 embryonated eggs of *T. muris*. **A**) Cells were isolated from the cecal lamina propria of uninfected or infected Veh and RAi treated mice, gated on $CD4^+$ $TCRb^+$ $Foxp3^-$cells and analyzed for intracellular GATA-3 expression. **B**) Total numbers of $GATA\text{-}3^+$ ILC (ILC2) and $CD4^+$ T cell (Th2). **C**) Worm burden in Veh or RAi treated mice 14 days after infection with *T. muris*. Data representative of three independent experiments with 4-5 mice in each experimental group. (Graphs display mean ±SEM).

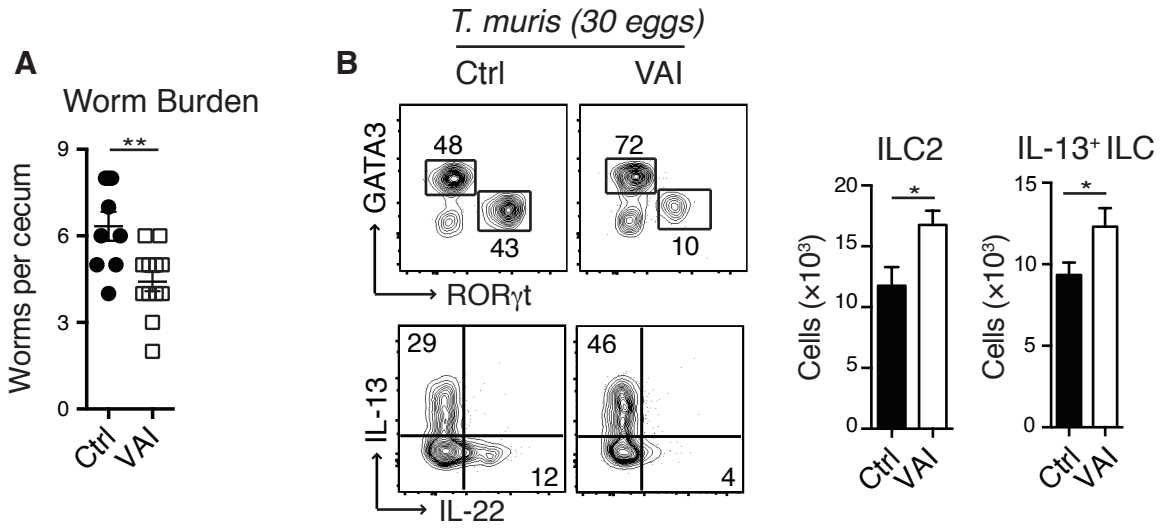

Fig. S21.
VAI mice show enhanced immunity and ILC2 responses during infection with *T. muris*. WT VAI and control (Ctrl) mice were infected with 30 embryonated *T. muris* eggs. **A**) Total number of worms in the cecum 13 days after infection. **B**) Cells were isolated from the lamina propria of the cecum of Ctrl or VAI WT mice 13 days after oral infection with T. muris. Cells were gated on Lin^-, $Thy1.2^+$ cells and analyzed for GATA3 and RORγt or IL-13 and IL-22 expression (left panel) and total number of ILC2 and $IL\text{-}13^+$ ILC (right panel). Data represent pooled data from two independent experiments with 3-6 mice in each experimental group. (Graphs display mean ±SEM).

A) ILC and CD4+ T cell gating (small intestinal lamina propria)

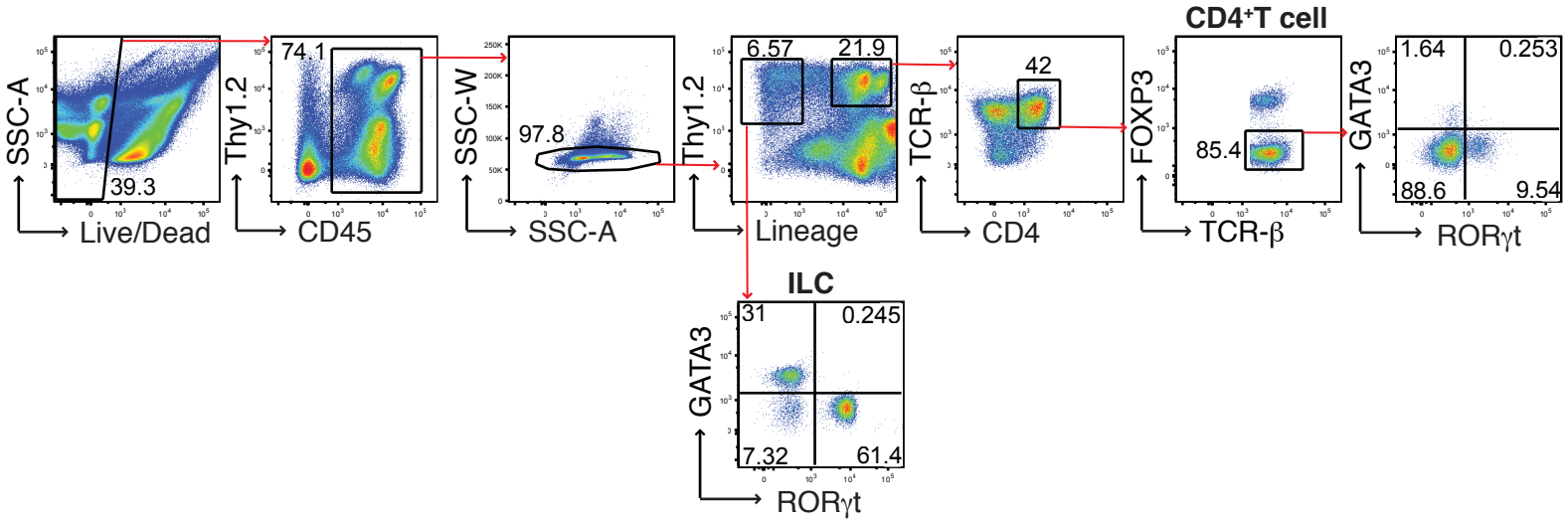

A) CLP/ILC2P sorting strategy (Bone marrow)

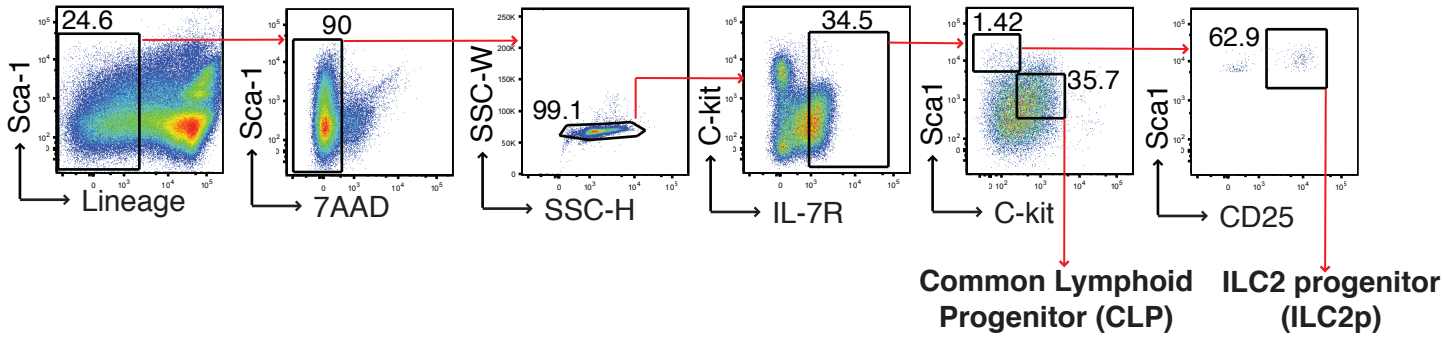

Fig. S22.
Gating strategy of cell populations A)ILC and CD4+ gating strategy for analysis of small intestinal lamina propria (siLP). B)Common lymphoid precursor (CLP) and ILC2 precursor(ILC2P) gating strategy from the bone marrow.

Table S1. mAB clones and suppliers

Antigen/Name	Clone	Fluorochrome	Supplier
CD11b	M1/70	Biotin, Pacific Blue	Biolegend/ebioscience
CD11c	N418	Biotin/PE-Cy7	ebioscience
CD19	6D5	Biotin	ebioscience
CD25	PC61	FITC/PE	ebioscience
CD4	RM4-5	AF700, Biotin	ebioscience
CD45	30-F11	APC-Cy7/PErcp-cy5.5	Biolegend/ebioscience
CD49b	DX5	Biotin	ebioscience
CD8b	ebioH35-17.2	Biotin	ebioscience
GR-1/Ly6G	RB6-8C5	FITC/Biotin	ebioscience
IL-13	eBio13a	FITC	ebioscience
IL-4	11B11	PE-Cy7	Biolegend
IL-5	TRFK5	PE	ebioscience
IL-9	RM9A4	AF647	Biolegend
IL-17A	Ebio17B7	BV605/PE/PerCP-Cy5.5	ebioscience
IL-22	IL22JOP	APC/ PerCP-eFluor 710	ebioscience
GMCSF	MP1-22E9	PE	ebioscience
IL-10	JES5-16E3	APC	ebioscience
IL-6	MP5-20F3	PE	ebioscience
MHCII	M5/114.15.2	AF700	ebioscience
NK1.1	PK136	Pacific Blue/Biotin	ebioscience
NKp46	29A1.4	APC	ebioscience
Sca-1	D7	Pacific Blue/FITC	Biolegend/ebioscience
Siglec F	E50-2440	PE	BD Biosciences
IL33R(T1/ST2)	DJ8	Biotin	MDbioproducts
TCRβ	H57-597	PerCP-Cy5.5/PE-Cy7	ebioscience
TCRγδ	GL3	Biotin	ebioscience
Ter-119	Ter119	Biotin	ebioscience
Thy1.2	30-H12	PE-Cy7/BV605	Biolegend
GATA3	L50-823	AF488/AF647	BD Biosciences
RORγt	B2D	PE/ PerCP-eFluor 710	ebioscience
T-bet	Ebio4B10	PE	ebioscience
Ki67	SolA15	FITC/PE-Cy7	ebioscience
CD127 (IL-7Rα)–Mouse	A7R34	PE-Cy7/APC	
CD45.1	A20	AF700/APC	ebioscience
CD45.2	104	APC/AF780	ebioscience
CD117 (c-Kit)	2B8	PE-Cy7/APC/ PErcp-cy5.5	ebioscience
Phospho-STAT5 (py694)	47/Stat5(pY694)	AF647	BD biosciences
KLRG1	2F1	PerCP-eFluor 710	ebioscience
CD127 (IL-7Rα)-Human	eBioRDR5	APC	ebioscience
Streptavidin		BV421	Biolegend

References

1. R. E. Ley, D. A. Peterson, J. I. Gordon, Ecological and evolutionary forces shaping microbial diversity in the human intestine. *Cell* **124**, 837–848 (2006).

2. World Health Organization, Soil-transmitted helminth infections (factsheet) (WHO, Geneva, 2013).

3. E. A. Kiss, C. Vonarbourg, S. Kopfmann, E. Hobeika, D. Finke, C. Esser, A. Diefenbach, Natural aryl hydrocarbon receptor ligands control organogenesis of intestinal lymphoid follicles. *Science* **334**, 1561–1565 (2011).

4. J. S. Lee, M. Cella, K. G. McDonald, C. Garlanda, G. D. Kennedy, M. Nukaya, A. Mantovani, R. Kopan, C. A. Bradfield, R. D. Newberry, M. Colonna, AHR drives the development of gut ILC22 cells and postnatal lymphoid tissues via pathways dependent on and independent of Notch. *Nat. Immunol.* **13**, 144–151 (2011).

5. Y. Li, S. Innocentin, D. R. Withers, N. A. Roberts, A. R. Gallagher, E. F. Grigorieva, C. Wilhelm, M. Veldhoen, Exogenous stimuli maintain intraepithelial lymphocytes via aryl hydrocarbon receptor activation. *Cell* **147**, 629–640 (2011).

6. J. Qiu, J. J. Heller, X. Guo, Z. M. Chen, K. Fish, Y. X. Fu, L. Zhou, The aryl hydrocarbon receptor regulates gut immunity through modulation of innate lymphoid cells. *Immunity* **36**, 92–104 (2012).

7. U. E. Schaible, S. H. Kaufmann, Malnutrition and infection: Complex mechanisms and global impacts. *PLOS Med.* **4**, e115 (2007).

8. WHO, Global Prevalence of Vitamin A Deficiency in Populations at Risk 1995–2005, WHO Global Database on Vitamin A Deficiency (WHO, Geneva, 2009).

9. J. A. Hall, J. R. Grainger, S. P. Spencer, Y. Belkaid, The role of retinoic acid in tolerance and immunity. *Immunity* **35**, 13–22 (2011).

10. M. Veldhoen, V. Brucklacher-Waldert, Dietary influences on intestinal immunity. *Nat. Rev. Immunol.* **12**, 696–708 (2012).

11. H. Spits, D. Artis, M. Colonna, A. Diefenbach, J. P. Di Santo, G. Eberl, S. Koyasu, R. M. Locksley, A. N. McKenzie, R. E. Mebius, F. Powrie, E. Vivier, Innate lymphoid cells—a proposal for uniform nomenclature. *Nat. Rev. Immunol.* **13**, 145–149 (2013).

12. H. Spits, J. P. Di Santo, The expanding family of innate lymphoid cells: Regulators and effectors of immunity and tissue remodeling. *Nat. Immunol.* **12**, 21–27 (2011).

13. B. Roediger, R. Kyle, K. H. Yip, N. Sumaria, T. V. Guy, B. S. Kim, A. J. Mitchell, S. S. Tay, R. Jain, E. Forbes-Blom, X. Chen, P. L. Tong, H. A. Bolton, D. Artis, W. E. Paul, B. Fazekas de St Groth, M. A. Grimbaldeston, G. Le Gros, W. Weninger, Cutaneous immunosurveillance and regulation of inflammation by group 2 innate lymphoid cells. *Nat. Immunol.* **14**, 564–573 (2013).

14. B. S. Kim, M. C. Siracusa, S. A. Saenz, M. Noti, L. A. Monticelli, G. F. Sonnenberg, M. R. Hepworth, A. S. Van Voorhees, M. R. Comeau, D. Artis, TSLP elicits IL-

33-independent innate lymphoid cell responses to promote skin inflammation. *Sci. Transl. Med.* **5**, 170ra16 (2013).

15. H. R. Cha, S. Y. Chang, J. H. Chang, J. O. Kim, J. Y. Yang, C. H. Kim, M. N. Kweon, Downregulation of Th17 cells in the small intestine by disruption of gut flora in the absence of retinoic acid. *J. Immunol.* **184**, 6799–6806 (2010).

16. J. A. Hall, J. L. Cannons, J. R. Grainger, L. M. Dos Santos, T. W. Hand, S. Naik, E. A. Wohlfert, D. B. Chou, G. Oldenhove, M. Robinson, M. E. Grigg, R. Kastenmayer, P. L. Schwartzberg, Y. Belkaid, Essential role for retinoic acid in the promotion of CD4(+) T cell effector responses via retinoic acid receptor alpha. *Immunity* **34**, 435–447 (2011).

17. P. Kastner, H. J. Lawrence, C. Waltzinger, N. B. Ghyselinck, P. Chambon, S. Chan, Positive and negative regulation of granulopoiesis by endogenous RARalpha. *Blood* **97**, 1314–1320 (2001).

18. C. Possot, S. Schmutz, S. Chea, L. Boucontet, A. Louise, A. Cumano, R. Golub, Notch signaling is necessary for adult, but not fetal, development of RORγt(+) innate lymphoid cells. *Nat. Immunol.* **12**, 949–958 (2011).

19. Q. Yang, S. A. Saenz, D. A. Zlotoff, D. Artis, A. Bhandoola, Cutting edge: Natural helper cells derive from lymphoid progenitors. *J. Immunol.* **187**, 5505–5509 (2011).

20. L. A. Mielke, S. A. Jones, M. Raverdeau, R. Higgs, A. Stefanska, J. R. Groom, A. Misiak, L. S. Dungan, C. E. Sutton, G. Streubel, A. P. Bracken, K. H. Mills, Retinoic acid expression associates with enhanced IL-22 production by γδ T cells and innate lymphoid cells and attenuation of intestinal inflammation. *J. Exp. Med.* **210**, 1117–1124 (2013).

21. G. F. Sonnenberg, L. A. Monticelli, M. M. Elloso, L. A. Fouser, D. Artis, CD4(+) lymphoid tissue-inducer cells promote innate immunity in the gut. *Immunity* **34**, 122–134 (2011).

22. A. A. Lima, R. L. Guerrant, Persistent diarrhea in children: Epidemiology, risk factors, pathophysiology, nutritional impact, and management. *Epidemiol. Rev.* **14**, 222–242 (1992).

23. E. Mayo-Wilson, A. Imdad, K. Herzer, M. Y. Yakoob, Z. A. Bhutta, Vitamin A supplements for preventing mortality, illness, and blindness in children aged under 5: Systematic review and meta-analysis. *BMJ* **343**, (aug25 1), d5094 (2011).

24. M. A. McGuckin, S. K. Lindén, P. Sutton, T. H. Florin, Mucin dynamics and enteric pathogens. *Nat. Rev. Microbiol.* **9**, 265–278 (2011).

25. J. A. Carman, C. E. Hayes, Abnormal regulation of IFN-gamma secretion in vitamin A deficiency. *J. Immunol.* **147**, 1247–1252 (1991).

26. U. Wiedermann, L. A. Hanson, H. Kahu, U. I. Dahlgren, Aberrant T-cell function in vitro and impaired T-cell dependent antibody response in vivo in vitamin A-deficient rats. *Immunology* **80**, 581–586 (1993).

27. M. Iwata, Y. Eshima, H. Kagechika, Retinoic acids exert direct effects on T cells to suppress Th1 development and enhance Th2 development via retinoic acid receptors. *Int. Immunol.* **15**, 1017–1025 (2003).

28. K. A. Hoag, F. E. Nashold, J. Goverman, C. E. Hayes, Retinoic acid enhances the T helper 2 cell development that is essential for robust antibody responses through its action on antigen-presenting cells. *J. Nutr.* **132**, 3736–3739 (2002).

29. G. U. Schuster, N. J. Kenyon, C. B. Stephensen, Vitamin A deficiency decreases and high dietary vitamin A increases disease severity in the mouse model of asthma. *J. Immunol.* **180**, 1834–1842 (2008).

30. K. J. Else, F. D. Finkelman, C. R. Maliszewski, R. K. Grencis, Cytokine-mediated regulation of chronic intestinal helminth infection. *J. Exp. Med.* **179**, 347–351 (1994).

31. A. J. Bancroft, A. N. McKenzie, R. K. Grencis, A critical role for IL-13 in resistance to intestinal nematode infection. *J. Immunol.* **160**, 3453–3461 (1998).

32. T. A. Wynn, IL-13 effector functions. *Annu. Rev. Immunol.* **21**, 425–456 (2003).

33. F. Chen, Z. Liu, W. Wu, C. Rozo, S. Bowdridge, A. Millman, N. Van Rooijen, J. F. Urban, Jr., T. A. Wynn, W. C. Gause, An essential role for T_H2-type responses in limiting acute tissue damage during experimental helminth infection. *Nat. Med.* **18**, 260–266 (2012).

34. B. Chapellier, M. Mark, J. M. Garnier, M. LeMeur, P. Chambon, N. B. Ghyselinck, A conditional floxed (loxP-flanked) allele for the retinoic acid receptor alpha (RARalpha) gene. *Genesis* **32**, 87–90 (2002).

35. C. M. Sun, J. A. Hall, R. B. Blank, N. Bouladoux, M. Oukka, J. R. Mora, Y. Belkaid, Small intestine lamina propria dendritic cells promote de novo generation of Foxp3 T reg cells via retinoic acid. *J. Exp. Med.* **204**, 1775–1785 (2007).

36. T. Hoyler, C. S. Klose, A. Souabni, A. Turqueti-Neves, D. Pfeifer, E. L. Rawlins, D. Voehringer, M. Busslinger, A. Diefenbach, The transcription factor GATA-3 controls cell fate and maintenance of type 2 innate lymphoid cells. *Immunity* **37**, 634–648 (2012).

37. A. Brickshawana, V. S. Shapiro, H. Kita, L. R. Pease, Lineage(-)Sca1+c-Kit(-)CD25+ cells are IL-33-responsive type 2 innate cells in the mouse bone marrow. *J. Immunol.* **187**, 5795–5804 (2011).

38. T. Y. Halim, A. MacLaren, M. T. Romanish, M. J. Gold, K. M. McNagny, F. Takei, Retinoic-acid-receptor-related orphan nuclear receptor alpha is required for natural helper cell development and allergic inflammation. *Immunity* **37**, 463–474 (2012).

39. G. Yang, L. Li, A. Volk, E. Emmell, T. Petley, J. Giles-Komar, P. Rafferty, M. Lakshminarayanan, D. E. Griswold, P. J. Bugelski, A. M. Das, Therapeutic dosing with anti-interleukin-13 monoclonal antibody inhibits asthma progression in mice. *J. Pharmacol. Exp. Ther.* **313**, 8–15 (2005).